



FIG. 3. Shearing interferometer pattern of pump, signal, and idler (conjugate) beams when disturbance is in the critical dimension.

Figure 3 shows shear patterns obtained when the rod is in the critical orientation. Here we use a rod 1.5 mm in diameter in order to provide a large region over which conjugation takes place. The shear is ~ 0.1 mm so that, unlike the previous example, the shear is only a small fraction of the size of the disturbance, and we can determine the size of the conjugating region directly from the shear plate. In this case, no more than 30% of the pattern can be conjugated, indicating an acceptance angle of 3×10^{-3} rad. Because of the limited size of the conjugation region, one sees only the middle of the S which is reflected about the interference lines of the pump when one goes from signal to conjugate.

In conclusion, we have demonstrated conjugation using a degenerate OPA. We are able to do this with modest pump powers of $\sim 10^3$ W in a collimated geometry, with conjugate intensities $\sim 0.5\%$ that of the signal, and conjugate-to-background intensity ratios of $10^3:1$. The conjugating process is limited by phase-match

considerations, with phase front tilts limited to $\sim 10^{-3}$ rad in the critical dimension and $\sim 10^{-2}$ rad in the non-critical case. In comparison, the cubic nonlinearity, while largely free of phase-match problems, requires much higher power densities than does the quadratic nonlinearity. For example, in CS_2 the gain² is $6 \times 10^{-3}SL$ (S is the flux in MW/cm^2 and L is the path length), whereas in $\text{LiCHO}_2 \cdot \text{H}_2\text{O}$ the gain is $0.27\sqrt{S}L$. With the $0.07\text{-MW}/\text{cm}^2$ flux density and 1-cm length used in the present work, CS_2 would have a gain of 0.4×10^{-3} (compared to 70×10^{-3} here) and conversion efficiency of signal to conjugate of 2×10^{-7} . Note that both ways of conjugating can, in principle, be considerably improved by using resonant enhancement² in the cubic case and by finding a more suitable crystal for the quadratic OPA. The latter is a complicated question which will be dealt with in a subsequent publication.

We gratefully acknowledge the help of J. Wyant, R. Shack, and H. van Driel. The assistance of B. Denton, C. Mah, J. Bessey, G. Al-Jumaily, and R. Sumner is also greatly appreciated.

¹A. Yariv, *J. Opt. Soc. Am.* 66, 301 (1976).

²R. Hellwarth, *J. Opt. Soc. Am.* 67, 1 (1977).

³B. Zel'dovich, V. Popovichev, V. Ragul'skii, and F. Faisullov, *JETP Lett.* 15, 109 (1972); O. Nosach, V. Popovichev, V. Ragul'skii, and F. Faisullov, *JETP Lett.* 16, 435 (1972).

⁴F. Zernike and J.E. Midwinter, *Applied Nonlinear Optics* (Wiley, New York, 1973), p. 42.

⁵S. Singh, W. Bonner, J. Potopowicz, and L. Van Uitert, *Appl. Phys. Lett.* 17, 292 (1970).

⁶M. Lurie, *Opt. Eng.* 15, 68 (1976).

A light-controlled light modulator^{a)}

D. Grischkowsky

IBM Thomas J. Watson Research Center, P.O. Box 218, Yorktown Heights, New York 10598
(Received 22 June 1977; accepted for publication 26 July 1977)

A fast resonantly enhanced light-controlled light modulator is demonstrated. Optical switching action is obtained with driving laser pulses with intensities as low as $2 \text{ kW}/\text{cm}^2$. The switching mechanism is the optical nonlinearity due to adiabatic following for the single photon resonance.

PACS numbers: 42.60.Fc, 42.65.Gv, 32.80.Kf

The idea of a light-controlled modulator has enjoyed a considerable amount of interest. The main appeal of these devices is their ability to transfer the amplitude modulation of one laser beam (the driving beam) to a second laser beam (the probing beam). This allows, in the case of a mode-locked driving beam, for amplitude modulation of the probing beam on the psec time scale.

The first demonstration of this situation was the ultra-fast light gate of Duguay and Hansen.¹ They used a strong driving beam to cause a Kerr liquid to become birefringent. The laser-induced birefringence caused a change of the polarization of the probing beam, and a switching action was obtained. This early demonstration required relatively high-intensity (approximately $100 \text{ MW}/\text{cm}^2$) driving beams and the time resolution was limited by the relaxation time of the Kerr liquid, typically many picoseconds.

Later Armstrong and Grischkowsky² proposed a dif-

^{a)}Work partially supported by the U.S. Office of Naval Research.

ferent approach using resonant enhancement in alkali vapors. In this approach which utilizes a circularly polarized driving beam that is nearly resonant with an atomic transition, it is possible for a relatively weak driving beam to switch a much more powerful probing beam. The basic idea of Ref. 2 is that the circularly polarized driving beam produces a coherent excitation³ (CE) in the near-resonant excited state. For most practical cases, the CE follows the intensity of the driving pulse. The change in atomic population due to CE causes the index of refraction to be different for right and left circularly polarized light, and the plane of polarization of the linearly polarized probing light will be rotated by passage through the vapor. This rotation will occur strongly for any frequency nearly resonant with the switching transition or nearly resonant with any other transition connected to either the ground or excited state of the switching transition.

The first demonstration of a resonantly enhanced modulator was performed by Liao and Bjorklund.^{4,5} In their innovative experiments, the laser-induced dispersion was caused by a two-photon resonance in atomic sodium vapor. For their case, the sum of the frequencies of the driving and probing beams is nearly resonant with a two-photon transition. This situation increases the sensitivity of the modulator enormously, compared to the Kerr liquids, and large rotation angles are obtained with driving beam intensities of typically 1 MW/cm². In addition, their complete theoretical discussion⁵ clarifies the role of the two-photon resonance and expands upon the somewhat oversimplified picture presented in Ref. 2.

In this paper, experimental results are presented for another situation described in Ref. 2, one where both the driving and probing pulses are nearly resonant with the same single-photon transition. For our example, both the driving and probing beams were obtained from the same 6-nsec-long dye laser pulse and counterpropagated through a rubidium vapor cell. The laser frequency was only 0.4 cm⁻¹ less than the resonant frequency of the strongly allowed $5S_{1/2} \rightarrow 5P_{1/2}$ transition (7948 Å) of rubidium. The small frequency offset allowed for a large rotation of the polarization of the probing beam due to passage through a 25-cm Rb vapor cell in the presence of a driving beam having an intensity of only 2 kW/cm². The rotation was found to be proportional to the intensity of the driving pulse. This feature verified that the adiabatic following nonlinearity was responsible for the rotation. By varying the time overlap between the probing and driving pulses, we

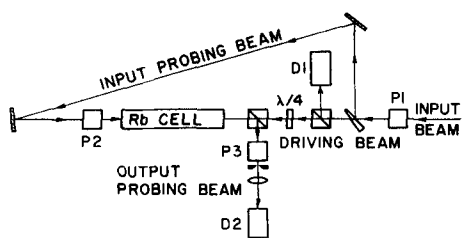


FIG. 1. Schematic diagram of the experiment.

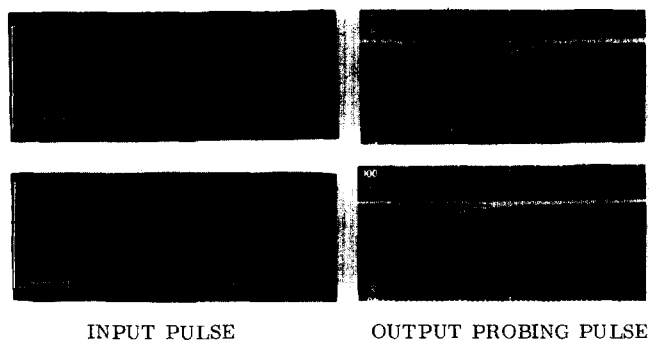


FIG. 2. Input pulses 5 nsec per large division. Output probing pulses 2 nsec per large division. (a) Driving pulse blocked from entering the Rb cell. Polarizer P3 rotated 10° from the position where P2 and P3 are crossed. (b) Polarizer P2 and P3 crossed. Input pulse corresponds to a driving pulse with a peak intensity of 1.6 kW/cm² entering the Rb cell.

were able to obtain switched output pulses which were shorter than the input pulses.

The schematic diagram of the experiment is shown in Fig. 1. The input beam is from a ruby-laser-pumped dye laser (DTTC in methanol) with a single-mode line-width of less than 0.005 cm⁻¹, a pulse width of 6 nsec, an output power of 400 W, and a beam diameter of 4 mm. After the input beam passes through polarizer P1, the probing beam is obtained by reflecting approximately 4% of the beam from a wedged glass plate. The driving beam is monitored by photodiode D1 and is circularly polarized by the quarter-wave plate. D1 is an ITT biplanar photodiode which drives a Tektronix 519 oscilloscope. The linearly polarized probing pulse enters the Rb cell from the opposite end after having passed through polarizer P2. After propagating through the Rb cell, part of the probing beam is reflected onto polarizer P3 which is usually crossed with respect to P2. If the polarization of the probing beam is rotated by passage through the cell, some of the beam will be transmitted through P3 and will be detected by D2, a Spectra-Physics 403 photodiode which drives a Tektronix 7904 oscilloscope.⁶ The 1-mm-diam aperture in front of the focusing lens for D2 restricts the monitored part of the probing beam to that which overlaps the central portion of the driving beam.

Figure 2 shows some experimental observations. For Fig. 2(a), the driving pulse was blocked from entering the Rb cell, and polarizer P3 was rotated 10° from the position where P2 and P3 were crossed. Thus, the output probing pulse shown is a replica of the input pulse with a magnitude corresponding to a 10° rotation. Figure 2(b) shows an optically switched probing pulse. Here, P2 and P3 were crossed, and the observed output pulse was due to the rotation of the polarization of the probing pulse by the driving pulse. Due to a reduction of 1/2 in the oscilloscope gain, the actual output pulse of Fig. 2(b) is approximately twice that of Fig. 2(a). Therefore, for Fig. 2(b) a portion of the probing pulse was rotated by about 15° by the driving pulse. By increasing the Rb atomic number density, it was possible to increase the switched pulse intensity to more than four times that of Fig. 2(b), corresponding to a rotation angle greater than 30°. As expected, the observed

magnitude of the switched pulse was independent of whether the input driving pulse was either σ^+ or σ^- light, and there was no switched pulse if the driving pulse was linearly polarized.

The rotation mechanism is the nonlinear index of refraction due to adiabatic following (AF).⁷ The AF nonlinearity has been well tested experimentally and has been shown to explain many self-action effects such as self-focusing, self-defocusing, and self-steepening. In essence, AF occurs when the light pulse is applied adiabatically with respect to the atomic resonance. The main condition is that the light pulse must change slowly compared to the period of the frequency offset. This condition is well satisfied here. Because the AF nonlinearity responds to the intensity of the applied light, the pulse shortening shown in Fig. 2(b) can be explained. For that case, the probing pulse was delayed with respect to the driving pulse by 4 nsec, thereby reducing the temporal overlap between the two pulses by the same amount. Consequently, one expects the output switched probing pulse to be shortened by about 4 nsec, which is in complete agreement with experiment.

We now calculate the rotation of the polarization of the probing beam, using the AF nonlinearity. The probing beam is considered to be the sum of two equal-intensity counterrotating circularly polarized beams designated as the σ^+ and the σ^- probing beams. The index of refraction for each beam is given by the expression

$$n_{\pm} = n_0 + n_2(\mathbf{E}_{\pm} \cdot \mathbf{E}_{\pm}), \quad (1)$$

where \mathbf{E}_{\pm} is the total σ^+ or σ^- electric field, n_0 is the linear index of refraction, and n_2 is the nonlinear component. Because we have restricted ourselves to the case where the driving beam is σ^+ light, we have the simple results that the indices of refraction for the σ^+ and σ^- probing beams are to a very good approximation equal to

$$n_+ = n_0 + n_2 \mathcal{E}_d^2, \quad (2a)$$

$$n_- = n_0 \quad (2b)$$

with \mathcal{E}_d (in esu) designating the electric field of the driving pulse, which is assumed to be much stronger than the probing pulse. The rotation angle Φ (in rad) of the polarization of the probing beam due to passage through the Rb cell is given by

$$\Phi = \pi l(n_+ - n_-)/\lambda, \quad (3a)$$

which is equivalent to

$$\Phi = \pi l n_2 \mathcal{E}_d^2 / \lambda, \quad (3b)$$

with

$$n_2 = 2\pi N_0 p_{12}^4 / (\hbar \Delta \omega)^3. \quad (3c)$$

In Eq. (3), $l = 25$ cm is the length of the Rb cell; $\lambda = 7948$ Å is the wavelength of the light; N_0 is the atomic number density in the $m_s = -\frac{1}{2}$ component of the $5S_{1/2}$ ground state of rubidium; $p_{12} = 6.16 \times 10^{-18}$ esu is the matrix element of the electric dipole moment for σ^+ light between the $5S_{1/2}$ and $5P_{1/2}$ states of Rb; $\Delta \omega = \omega_0 - \omega$, where ω_0 is the resonant angular frequency and ω is the

angular frequency of the laser.

We can now calculate Φ for the situation of Fig. 2(b), where the peak driving pulse intensity was 1.6 kW/cm², $N_0 = 0.3 \times 10^{13}$ /cm³ corresponding to the cell temperature of 100 °C, and the frequency offset was $(\Delta \omega / 2\pi c) = 0.4$ cm⁻¹. Using these experimental parameters, we calculate Φ to be 20° which is close to the measured value of 15° . It is interesting to compare our calculated nonlinear coefficient $n_2 = -0.5 \times 10^{-7}$ with that for CS₂, one of the most nonlinear Kerr liquids, for which $n_2 = 2 \times 10^{-11}$ esu. It is this tremendous difference in the strengths of the nonlinearity that allows us to switch pulses with kW/cm² intensities rather than the MW/cm² intensities required for the Kerr liquids.

Roughly speaking, the time response of the modulator is limited to the period of the frequency offset of the driving beam from the resonance line, i.e., for an offset of 10 cm⁻¹ the modulator switching speed will be about 3 psec. It should be clear that there is no requirement that the probing and driving beams counter-propagate or that they have the same frequency. By using counterpropagating beams, it is easier to separate the driving and probing beams when the frequencies are the same or only slightly different. However, the modulator response time is then also limited by the transit time through the vapor cell. Therefore, when mode-locked driving pulses are used and psec response times are desired, it is essential that both the driving and probe beams propagate through the vapor cell in the same direction, unless of course, the cell dimensions are appropriately reduced. Probably, the most useful case will be when the frequencies of the probing and driving beams are different. For this case, the resonant denominator of n_2 given in Eq. (3c) changes to $(\Delta \omega)^2 \Delta \omega_p$ with $\Delta \omega_p = \omega_0 - \omega_p$, where ω_p is the probing frequency. When the driving frequency is much closer to the resonance than the probing frequency, the intensity of the driving beam can be much less than that of the probing beam. Therefore, it becomes possible for a driving beam to switch a probing beam as much as a thousand times more powerful, and a type of optical transistor action can be achieved.²

I would like to acknowledge careful readings of this manuscript by D.S. Bethune, R.T. Hodgson, M.M.T. Loy, and P.P. Sorokin. Also, the expert technical support of R.J. Bennett was important to this work.

¹M.A. Duguay and J.W. Hansen, Appl. Phys. Lett. **15**, 192 (1969).

²J.A. Armstrong and D. Grischkowsky, U.S. Patent No. 3,864,020 (1975).

³D. Grischkowsky, Phys. Rev. A **14**, 802 (1976).

⁴P.F. Liao and G.C. Bjorklund, Phys. Rev. Lett. **36**, 584 (1976).

⁵P.F. Liao and G.C. Bjorklund, Phys. Rev. A **15**, 2009 (1977).

⁶The Rb cell axis is tilted with respect to the driving and probing beams so that the reflection of the driving beam from the input window of the cell is not parallel to the output probing beam. Consequently, in the focal plane of the lens, in front of the detector D2, the focal spots of the reflected driving beam and the probing beam are well separated

from each other. Because the D2 detector element is small compared to the separation between the two focal spots of the probing beam, only the probing beam is monitored, when D2 is centered on the focal spot of the probing beam.

[†]D. Grischkowsky, Phys. Rev. Lett. **24**, 866 (1970); D. Grischkowsky and J. A. Armstrong, Phys. Rev. A **6**, 1566 (1972); D. Grischkowsky, Eric Courtens, and J. A. Armstrong, Phys. Rev. Lett. **31**, 422 (1973).

An infrared upconverter for astronomical imaging^{a)}

R. W. Boyd and C. H. Townes

Department of Physics, University of California, Berkeley, California 94720
(Received 5 July 1977; accepted for publication 28 July 1977)

An imaging upconverter has been constructed which is suitable for use in the study of the thermal 10- μm radiation from astronomical sources. The infrared radiation is converted to visible radiation by mixing in a 1-cm-long proustite crystal. The phase-matched 2-cm⁻¹ bandpass is tunable from 9 to 11 μm . The conversion efficiency is 2×10^{-7} , and the field of view of 40 arc seconds on the sky contains several hundred picture elements, approximately diffraction-limited resolution in a large telescope. The instrument has been used in studies of the sun, moon, Mercury, and VY Canis Majoris.

PACS numbers: 42.80.Qy, 42.65.Cq, 95.85.Gn, 95.75.Mn

There has long been interest in utilizing upconversion as a means of converting images from infrared wavelengths to the visible region where convenient image storage devices (such as photographic films) are readily available.¹ This letter describes an imaging upconverter with sufficient sensitivity that it has been used to study the thermal 10- μm radiation from several astronomical objects. This represents the first successful application of imaging upconversion to astronomy and, while of limited efficiency, demonstrates the promise of such devices when larger nonlinear optical responses are developed.

The requirements on an upconversion system for astronomy are different from those for some other purposes in that the primary needs are a good time-averaged conversion efficiency and diffraction-limited angular resolution over a field of view. Thus, the high conversion efficiencies obtainable by pulsed techniques are not necessarily advantageous, and efficiency must also be compromised in order to obtain a number of converted picture elements. Fortunately, most astronomical applications require only a rather small field of view at the telescope, but wave-front distortion must be avoided in order to approach the maximum resolution allowed by diffraction from the telescope aperture. In addition to these qualities, good spectral resolution is sometimes needed for astronomical applications.

The upconversion process is well understood,² and only a brief description of it will be given here. The apparatus is shown in Fig. 1. Infrared radiation is collected with an $f/56$ optical system, which is arranged so as to form an exit pupil at the center of a 1-cm-long nonlinear proustite crystal. The infrared radiation is collimated at the crystal, so that each point in the image space of the upconverter is represented at the

crystal by a plane wave of a distinct propagation direction. The infrared signal is then mixed with a 0.25-W 0.7525- μm wavelength krypton ion laser beam. A simple grating monochromator was constructed to spectrally separate the laser frequency from the broadband light of the laser discharge tube. A grating monochromator was selected for this purpose in order to avoid the problem of fluorescence which accompanied the use of glass filters. The laser beam is injected into the cone of infrared radiation through a hole in the infrared collimating mirror.

The laser and infrared beams mix in the proustite crystal, generating an optical signal at the sum frequency. Type-II phase matching³ is used to avoid an absorption feature for the ordinary ray at 10 μm in proustite. The upconverter can be conveniently angle tuned from 9 to 11 μm . The quantum conversion efficiency of infrared photons into visible-frequency photons is given by⁴

$$\eta = \frac{512\pi^5 d_{\text{eff}}^2 I_L}{n_{\text{IR}} n_L n_S \lambda_S \lambda_{\text{IRC}}} \left(\frac{\sin \frac{1}{2} l \Delta k}{\frac{1}{2} \Delta k} \right)^2, \quad (1)$$

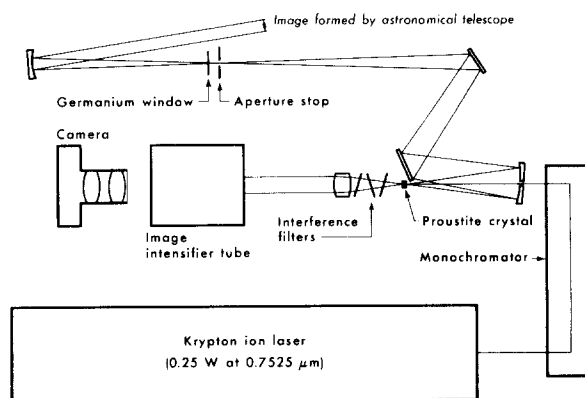


FIG. 1. Optical layout of the 10- μm imaging upconverter.

^{a)}Work partially supported by NASA Grants NGL 05-003-272 and NGR 05-003-452.